

Glacier shrinkage in the Alps continues unabated as revealed by a new glacier inventory from Sentinel-2

Frank Paul¹, Philipp Rastner¹, Roberto Sergio Azzoni², Guglielmina Diolaiuti², Davide Fugazza², Raymond Le Bris¹, Johanna Nemeč³, Antoine Rabatel⁴, Mélanie Ramusovic⁴, Gabriele Schwaizer³, Claudio Smiraglia²

1 Department of Geography, University of Zurich, Zurich, Switzerland

2 Department of Environmental Science and Policy, University of Milan, Milan, Italy

3 ENVEO IT GmbH, Innsbruck, Austria

4 Univ. Grenoble Alpes, CNRS, IRD, Grenoble-INP, Institut des Géosciences de l'Environnement (IGE, UMR5001), Grenoble, France

Correspondence: Frank Paul (frank.paul@geo.uzh.ch)

Abstract

The on-going glacier shrinkage in the Alps requires frequent updates of glacier outlines to provide an accurate database for monitoring, modeling purposes (e.g. determination of run-off, mass balance, or future glacier extent) and other applications. With the launch of the first Sentinel-2 (S2) satellite in 2015, it became possible to create a consistent, Alpine-wide glacier inventory with an unprecedented spatial resolution of 10 m. Already the first S2 images from August 2015 provided excellent mapping conditions for most glacierised regions in the Alps and were used as a base for the compilation of a new Alpine-wide glacier inventory in a collaborative team effort. In all countries, glacier outlines from the latest national inventories have been used as a guide to compile an update consistent with the respective previous interpretation. The automated mapping of clean glacier ice was straightforward using the band ratio method, but the numerous debris-covered glaciers required intense manual editing. Cloud cover over many glaciers in Italy required including also S2 scenes from 2016. The outline uncertainty was determined with multiple digitising of 14 glaciers by all participants. Topographic information for all glaciers was obtained from the ALOS AW3D30 DEM. Overall, we derived a total glacier area of $1806 \pm 60 \text{ km}^2$ when considering 4395 glaciers $>0.01 \text{ km}^2$. This is 14% (-1.2%/a) less than the 2100 km^2 derived from Landsat in 2003 and indicating an unabated continuation of glacier shrinkage in the Alps since the mid-1980s. It is a lower bound estimate, as due to the higher spatial resolution of S2 many small glaciers were additionally mapped or increased in size compared to 2003. Median elevations peak around 3000 m a.s.l. with a high variability that depends on location and aspect. The uncertainty assessment revealed locally strong differences in interpretation of debris-covered glaciers, resulting in limitations for change assessment when using glacier extents digitised by different analysts. The inventory is available at: doi.pangaea.de/10.1594/PANGAEA.909133 (Paul et al., 2019).

fp 28 4 20 3:19 PM

Deleted: or

fp 28 4 20 3:19 PM

Deleted: Fortunately, already

fp 28 4 20 3:19 PM

Deleted: acquired in

fp 28 4 20 3:19 PM

Deleted: of the

fp 28 4 20 3:19 PM

Deleted: . We have

fp 28 4 20 3:19 PM

Deleted: this opportunity to compile

fp 28 4 20 3:19 PM

Deleted: a

fp 28 4 20 3:19 PM

Deleted: update. However, cloud cover over many glaciers in Italy required including also S2 scenes from 2016. Whereas the

fp 28 4 20 3:19 PM

Deleted: The

fp 28 4 20 3:19 PM

Deleted: in the outlines

fp 28 4 20 3:19 PM

Deleted: derived

fp 28 4 20 3:19 PM

Deleted: 4394

fp 28 4 20 3:19 PM

Deleted: scenes acquired

fp 28 4 20 3:19 PM

Deleted: Due

fp 28 4 20 3:19 PM

Deleted: in the new inventory

fp 28 4 20 3:19 PM

Deleted: An artificial reduction to the former extents would thus result in an even higher overall area loss. Still, the

fp 28 4 20 3:19 PM

Deleted: considerable

fp 28 4 20 3:19 PM

Deleted: <https://doi.pangaea.de/10.1594/PANGAEA.909133>.

61

62 | 1. Introduction

63 Precise information on glacier extents is required for numerous glaciological and hydrological cal-
64 culations, ranging from the determination of glacier volume, surface mass balance and future glac-
65 ier evolution to run-off, hydro-power production, and sea-level rise (e.g., Marzeion et al., 2017).
66 For these and several other applications glacier outlines spatially constrain all calculations thus
67 providing an important baseline dataset. In response to the on-going atmospheric warming, glaci-
68 ers retreat, shrink and lose mass in most regions of the world (e.g., Gardner et al. 2013, Wouters et
69 al. 2019, Zemp et al. 2019). Accordingly, a frequent update of glacier inventories is required to
70 reduce uncertainties in subsequent calculations. With relative area loss rates of about 1% per year
71 in many regions globally (Vaughan et al. 2013), glaciers lose about 10% of their area within a dec-
72 ade and a decadal update frequency seems sensible. In regions with stronger glacier shrinkage such
73 as the tropical Andes (e.g. Rabatel et al. 2013, 2018) or the European Alps (e.g. Gardent et al.
74 2014) an even higher update frequency is likely required. However, apart from the high workload
75 required to digitise or manually correct glacier outlines (e.g. Racoviteanu et al. 2009), it is often
76 not possible to obtain satellite images in a desired period of the year with appropriate mapping
77 conditions, i.e. without seasonal snow and clouds hiding glaciers. Hence, glacier inventories are
78 often compiled from images acquired over several years resulting in a temporarily inhomogeneous
79 dataset. Fortunately, a 3-year period of acquisition is still acceptable in error terms, as area chang-
80 es of about $\pm 3\%$ are within the typical area uncertainty of about 3 to 5% (e.g. Paul et al. 2013).

81

82 The last glacier inventory covering the entire Alps with a common and homogeneous date was
83 compiled from Landsat Thematic Mapper (TM) images acquired within six weeks in the summer
84 of 2003 (Paul et al. 2011). Although this dataset has its caveats (e.g. missing small glaciers in Italy
85 and some debris-covered ice), it is methodologically and temporarily consistent and represents
86 glacier outlines of the Alps in the Randolph Glacier Inventory (RGI). A few years later, high quali-
87 ty glacier inventories were compiled from very high-resolution datasets (aerial photography, air-
88 borne laser scanning) on a national level in all four countries of the Alps with substantial glacier
89 coverage (Austria, France, Italy, Switzerland). These more recent inventories refer to the periods
90 2008-2011 for Switzerland (Fischer et al. 2014), 2004-2011 for Austria (Fischer et al. 2015), 2006-
91 2009 for France (Gardent et al. 2014), and 2005-2011 for Italy (Smiraglia et al. 2015). As an 8-
92 year period is rather long, consistent and comparable change assessment is challenging. However,
93 for the first version of the World Glacier Inventory (WGI) the temporal spread was even larger,
94 ranging from 1959 to about 1983 (Zemp et al. 2008). Another problem for change assessment is
95 the inhomogenous interpretation of glacier extents that occurs in part to be compliant with the in-
96 terpretation in earlier national inventories. Hence, calculations over the entire Alps that require a
97 consistent time stamp are difficult to perform and rates of glacier change are difficult to compare
98 across regions (e.g. Gardent et al. 2014).

fp 28 4 20 3:19 PM

Deleted:

fp 28 4 20 3:19 PM

Deleted: 2

fp 28 4 20 3:19 PM

Deleted: has been

fp 28 4 20 3:19 PM

Deleted: representing

fp 28 4 20 3:19 PM

Deleted: ,

fp 28 4 20 3:19 PM

Deleted: analysis

105

106 Considering the on-going strong glacier shrinkage in the Alps over the past decades and the above
107 shortcomings of existing datasets, there is a high demand to compile a (1) new, (2) precise and (3)
108 consistent glacier inventory for the entire Alps, with data acquired under (4) good mapping condi-
109 tions in (5) a single year. Although it might be difficult to satisfy all five criteria at the same time,
110 at least some of them seem achievable by means of recently available satellite data. With the 10 m
111 resolution data from Sentinel-2 (S2) and its 290 km swath width it is possible (a) to improve the
112 quality of the derived glacier outlines (compared to Landsat TM) substantially (Paul et al. 2016)
113 and (b) to cover a region such as the Alps with a few scenes acquired within a few weeks or even
114 days, satisfying criteria (2) and (5). Good mapping conditions, however, only occur by chance af-
115 ter a comparably warm summer when all seasonal snow off glaciers has melted and largely cloud
116 free conditions persist over an extended time span in August or September.

117

118 In this study we present a new glacier inventory for the European Alps that has been compiled
119 from S2 data that were mostly acquired within two weeks of August 2015 (during the commission-
120 ing phase). However, due to glaciers (mostly in in Italy) being partly cloud-covered, also scenes
121 from 2016 (and very few from 2017) were used. Hence, criterion (5) could not be fully satisfied. In
122 order to satisfy point (3), we decided to perform the mapping of clean ice with an identical method
123 (band ratio), and distribute the raw outlines to the national experts for editing of wrongly classified
124 regions (e.g. adding missing ice in shadow and under local clouds or debris cover, removing lakes
125 and other water surfaces). As a guide for the interpretation the analysts used the latest high-
126 resolution inventory in each country. All corrected datasets were merged into one dataset and
127 topographic information for each glacier was derived from the ALOS AW3D30 DEM. For uncer-
128 tainty assessment all participants corrected the extents of 14 glaciers independently four times.

129

130 **2. Study region**

131 The Alps are a largely west-east (south-north in the West) oriented mountain range in the centre of
132 Europe (roughly from 2° to 18° E and 43° to 49° N) with peaks reaching 4808 m a.s.l. in the West
133 at Mt. Blanc/Monte Bianco and elevations above 3000 m a.s.l. in most regions. In Fig. 1 we show
134 the region covered by glaciers along with footprints of the tiles used for data processing. The Alps
135 act thus as a topographic barrier for air masses coming from the North and South ([Auer et al.](#)
136 [2007](#)) as well as from the West in the western part. This results in enhanced orographic precipita-
137 tion and a high regional variability of precipitation amounts in specific years as well as in the long-
138 term mean (e.g. Frei et al. 2003). On the other hand, temperatures are horizontally rather uniform
139 (e.g. Böhm et al. 2001) but vary strongly with height according to the atmospheric lapse rate (e.g.
140 Frei 2014). Snow accumulation is mostly due to winter precipitation, but some snowfall can also
141 occur in summer at higher elevations, reducing ablation for a few days.

142

143 There is no significant long-term trend in precipitation over the last 100+ years (Casty et al. 2005),
 144 but summer temperatures in the Alps have increased sharply (by about 1 °C) in the mid-1980s (e.g.
 145 Beniston 1997, Reid et al. 2016). In consequence, winter snow cover barely survives the summer
 146 even at high elevations and / or when strong positive deviations in temperature occurred. Glacier
 147 mass balances in the Alps were thus pre-dominantly negative over the past three decades (e.g.
 148 Zemp et al. 2015) and the related mass loss resulted in widespread glacier shrinkage and disinte-
 149 gration over the past decades (e.g. Gardent et al. 2014, Paul et al. 2004). [An order of magnitude](#)
 150 [estimate with a rounded](#) total area of about 2000 km² in 2003 and a mean annual [specific](#) mass loss
 151 of [1 m w.e. per year](#) (e.g. Zemp et al. 2015), [gives a loss of](#) about 2 Gt of ice per year [in the Alps](#).

152
 153 Most glaciers in the Alps are of cirque, mountain and valley type and the two largest ones (Aletsch
 154 and Gorner glaciers) have an area of about 80 km² and 60 km², respectively. Some glaciers reach
 155 down to 1300 m a.s.l., and the overall mean elevation is around 3000 m a.s.l., a unique value com-
 156 pared to other regions of the RGI (e.g. Pfeffer et al. 2014). Due to the surrounding often ice-free
 157 rock walls of considerable height, many glaciers in the Alps are heavily debris-covered. Whereas
 158 this allowed the tongues of several large valley glaciers to survive at comparably low elevations
 159 (Mölg et al. 2019), many glaciers - large and small - become [hidden](#) under increasing amounts of
 160 debris. Combined with the on-going down-wasting and disintegration, precisely mapping their ex-
 161 tents is increasingly challenging.

Figure 1

3. Datasets

3.1 Satellite data

167 In total, [17 unique S2 tiles](#) [from 8 different dates](#) were processed to cover the study region with
 168 cloud free images (Figure 1 and Table 1). [These are split among the 4 countries resulting in 29 in-](#)
 169 [dependently processed image footprints](#). Of these, [15](#) were acquired in 2015, [11](#) in 2016 and 3 in
 170 2017. Convective clouds in Italy (mostly along the Alpine main divide) required [extending](#) the
 171 main acquisition period over two years. All glaciers in France were mapped from four tiles ac-
 172 quired on 29.8.2015. This date covers also most glaciers mapped in Switzerland (five tiles) apart
 173 from the south-east tile 32TNS (ID: 11) that was acquired three days earlier (26.8.2015). [Two tiles](#)
 174 from that date (32TNT/TPT) are used to map glaciers in western-Austria and three tiles
 175 (32TQT/TQS and 33TUN) from 27.8.2016 for the eastern part of Austria. Twelve tiles [cover the](#)
 176 glaciers in Italy, [seven from 2016](#), and [in total five from 2015 and 2017](#) (Fig. 1). However, [those](#)
 177 [from 2017](#) only cover very few and small glaciers so that collectively the northern (Switzerland /
 178 Austria) and western (France) parts of the inventory are from 2015 whereas the southern (Italy)
 179 and eastern (Austria) parts are from 2016. All tiles were downloaded from remotepixel.ca (only
 180 the required bands, [this is](#) no longer possible), earthexplorer.usgs.gov or the Copernicus Hub.

fp 28 4 20 3:19 PM
 Deleted: With a

fp 28 4 20 3:19 PM
 Deleted: about

fp 28 4 20 3:19 PM
 Deleted: , the European Alps currently lose

fp 28 4 20 3:19 PM
 Deleted: invisible

fp 28 4 20 3:19 PM
 Deleted: 23

fp 28 4 20 3:19 PM
 Deleted: 11

fp 28 4 20 3:19 PM
 Deleted: 9

fp 28 4 20 3:19 PM
 Deleted: stretching

fp 28 4 20 3:19 PM
 Deleted: Three

fp 28 4 20 3:19 PM
 Deleted: / TNS /

fp 28 4 20 3:19 PM
 Deleted: / 32TQS /

fp 28 4 20 3:19 PM
 Deleted: had to be used to map

fp 28 4 20 3:19 PM
 Deleted: of which two are from 2015

fp 28 4 20 3:19 PM
 Deleted: are

fp 28 4 20 3:19 PM
 Deleted: ,

fp 28 4 20 3:19 PM
 Deleted: three

fp 28 4 20 3:19 PM
 Deleted: the latter three

fp 28 4 20 3:19 PM
 Deleted: Open Access

199

200

201

Table 1

202 From all tiles, bands 2, 3, 4, 8, and 11 (blue, green, red, Near Infra-Red / NIR, Short Wave Infra-
203 Red / SWIR) of the sensor Multi Spectral Imager (MSI) were downloaded and colour composites
204 were created from the 10 m visible and NIR (VNIR) bands. The 20 m SWIR band 11 was bilinear-
205 ly resampled to 10 m resolution to obtain glacier outlines at this resolution. The 10 m resolution
206 VNIR bands allowed for a much better identification of glacier extents (e.g. correcting debris-
207 covered parts) than possible with Landsat (Paul et al. 2016), resulting in a higher quality of the
208 outlines. Apart from the resampling, all image bands are used as they are except for Austria, where
209 further pre-processing has been applied (see Section 4.2.1). The August 2015 scenes from the S2
210 commissioning phase had reflectance values stretched from 1 to 1000 (12 bit) instead of the later
211 16 bit (allowing values up to 65536), but this linear rescaling had no impact on the threshold value
212 for the band ratio (see Section 4.1).

213

214 **3.2 Digital elevation models (DEMs)**

215 We originally intended using the new TanDEM-X (TDX) DEM to derive topographic information
216 for all glaciers, as it covers the entire Alps and was acquired closest (around 2013) to the satellite
217 images used to create the inventory. However, closer inspection revealed that it had data voids and
218 suffered from severe artefacts (Fig. 2). Although these are mostly located in the steep terrain out-
219 side of glaciers, many smaller glaciers are severely impacted, resulting in wrong topographic in-
220 formation. As an alternative we investigated the ALOS AW3D30 DEM that was compiled from
221 ALOS tri-stereo scenes (Takaku et al. 2014) and acquired about five years before the TDX DEM
222 (around 2008). The AW3D30 DEM has a less good temporal match but no data voids and compar-
223 ably few artefacts (Fig. 2). The individual tiles were merged into one 30 m dataset in UTM 32N
224 projection with WGS84 datum. For the pre-processing of satellite bands in Austria, a national
225 DEM with 10 m resolution derived from laser scanning was used (Open Data Österreich: da-
226 ta.gv.at).

227

Figure 2

228

229

230 **3.3 Previous glacier inventories**

231 As mentioned above, outlines from previous national glacier inventories were used to guide the
232 delineation. They have been mostly compiled from aerial photography with very high spatial reso-
233 lution (better than 1 m) and should thus provide the highest possible quality. This allowed consid-
234 ering very small and otherwise unnoticed glaciers and helped to identify glacier zones that are de-
235 bris covered. The substantial glacier retreat that took place between the two inventories was well
236 visible in most cases and did not hamper the interpretation. However, a larger number of very
237 small glaciers were not mapped in 2003 and have now been added or digitised with larger extents.

238 A large issue with respect to additional work load is the compilation of ice divides. They can be
239 derived semi-automatically from watershed analysis of a DEM using a range of methods (e.g.
240 Kienholz et al. 2013), but in general numerous manual corrections have still to be applied. To pro-
241 vide some consistency with previous national inventories, we decided [to use](#) the drainage divides
242 from these inventories to separate glacier complexes into entities. However, due to the locally poor
243 geolocation of the S2 scenes (Kääb et al. 2016, Stumpf et al. 2018) [some ice divides of the former](#)
244 [inventories overlapped with glacier extents and were](#) manually adjusted.

fp 28 4 20 3:19 PM
Deleted: using

fp 28 4 20 3:19 PM
Deleted:), the location of the

fp 28 4 20 3:19 PM
Deleted: was partly

246 4. Methods

247 4.1 Mapping of clean ice in all regions

248 Automated mapping of clean to slightly dirty glacier ice is straight forward using a red or NIR to
249 SWIR band ratio and a (manually selected) threshold (e.g. Paul et al. 2002). Also other methods
250 such as the normalised difference snow index (NDSI) work well (e.g. Racoviteanu et al. 2009) as
251 both utilise the strong difference in reflectance from the VNIR to the SWIR for snow and ice (e.g.
252 Dozier 1989). As the latter are bright in the VNIR bands (high reflectance) but very dark (low re-
253 flectance) in the SWIR, dividing a VNIR band by a SWIR band gives high values over glacier ice
254 and snow and very low ones over all other terrain as this is often much brighter in the SWIR than
255 the VNIR. The manual selection of a threshold for each scene (or S2 tile) has the advantage to in-
256 clude a regional adjustment of the threshold to local atmospheric conditions. We followed the rec-
257 ommendation to select the threshold in a way that good mapping results in regions with shadow
258 are achieved. By lowering the threshold, more and more [rock in shadow](#) is included, creating a
259 [noisy result](#). It has been shown [by Paul et al. \(2016\)](#) that glacier mapping with S2 (using a red /
260 SWIR ratio) requires an additional threshold in the blue band to remove misclassified rock in
261 shadow [\(that can have the same ratio value as ice in shadow but is darker in the blue band\)](#). Hence,
262 for this inventory glaciers have been first automatically identified following the equation:

fp 28 4 20 3:19 PM
Deleted: bare

fp 28 4 20 3:19 PM
Deleted: very

fp 28 4 20 3:19 PM
Deleted: in a previous study (

fp 28 4 20 3:19 PM
Deleted: .

$$(red / SWIR) > th1 \text{ and } blue > th2$$

266 with the empirically derived thresholds $th1$ and $th2$. As mentioned above, the SWIR band was bi-
267 linearly resampled from 20 to 10 m spatial resolution before computing the ratio. No filter for im-
268 age smoothing was applied to retain fine spatial details, such as rock outcrops. Figure 3 shows for
269 a test site in the Mt. Blanc region (Leschaux Glacier) the impact of the threshold selection. Figure
270 3a depicts the (contrast stretched) red / SWIR ratio image, Fig. 3b the impact of $th1$ on the mapped
271 area, Fig. 3c the impact of $th2$, and Fig. 3d the resulting outlines after raster-vector conversion. As
272 can be seen in Fig. 3b, there is very little impact on the mapped glacier area when increasing $th1$
273 in steps of 0.2. For this region we used 3.0 as $th1$ resulting in the blue and yellow areas as the
274 mapped glacier. Wrongly mapped rock in shadow is then reduced back with $th2$ (Fig. 3c). In this

282 case a value of 860 was selected for *th2* i.e. only the blue area is considered. This correctly re-
283 moved rock in shadow from the glacier mask for the region to the right of the white arrow but, on
284 the other hand, correctly mapped ice in shadow is removed at the same time in the region above
285 the green arrow (Figs. 3c and d). Hence, threshold selection is always a compromise as it is in gen-
286 eral not possible to map everything correctly with one set of thresholds. The resulting glacier maps
287 for all regions were converted to a shape file using raster-vector conversion and by setting the non-
288 glacier class to 'no data' before. In the resulting shape file internal rocks are thus data voids.

289
290 All pre-processed scenes were provided in their original geometry for correction by the national
291 experts. As shown in Fig. 3c, it was sometimes not possible to include dark bare ice and at the
292 same time exclude bare rock in shadow. Such wrongly classified regions were corrected by the
293 analysts together with data gaps for debris cover and clouds (omission errors), wrongly mapped
294 water bodies (e.g. turbid lakes and rivers) and shadow regions (commission errors). By setting the
295 minimum glaciers size to 0.01 km², most of the often very small snow patches were removed, (cf.
296 [Leigh et al. 2019](#)).

297
298 *Figure 3*

300 4.2 Corrections in the different countries

301 4.2.1 Austria

302 The satellite scenes for Austria were further pre-processed by [G. Schwaizer](#) (cf. Paul et al. 2016) to
303 remove water surfaces and improve classification of glacier ice in cast shadow, before manual cor-
304 rections were applied. The latter work was mainly performed by one person (J. Nemeč). Two pre-
305 vious Austrian glacier inventories (Lambrecht and Kuhn 2007, Fischer et al. 2015) were used to
306 support the interpretation of small glaciers, debris covered glacier parts, and the boundary across
307 common accumulation areas. Further, an internal independent quality control of the generated
308 glacier outlines was made by a second person (G. Schwaizer), using orthophotos (30 cm pixel
309 spacing) acquired in late August 2015 for most Austrian glaciers for overall accuracy checks and
310 to assure the correct delineation of debris covered glacier areas. In Fig. 4a we illustrate the strong
311 glacier shrinkage from 1998 (yellow lines) to 2016 (red) as well as the manual corrections applied,
312 extending the bright filled areas of the raw classification to the red extents.

314 4.2.2 France

315 The raw glacier outlines from S2 were corrected by one person (A. Rabatel). The glacier outlines
316 from the previous inventory by Gardent et al. (2014) were used for the interpretation, in particular
317 in shadow regions and for glaciers under debris cover. It is noteworthy that the previous inventory
318 was made on the basis of aerial photographs (2006-2009) with field campaigns for the debris-
319 covered glacier tongues to clarify the outline delineation. As a consequence, this previous invento-
320 ry constitutes a highly valuable reference. In addition, because even on debris-covered glaciers the

fp 28 4 20 3:19 PM

Deleted: .

fp 28 4 20 3:19 PM

Deleted: (see

323 | changes between 2006-09 and 2015 are [visible](#) (Fig. 4b), Pléiades images from 2015-2016 ac-
324 | quired within the KALIDEOS-Alpes / CNES program were use as a guideline, mostly for the
325 | heavily debris-covered glacier tongues.

326 | 327 | 4.2.3 Italy

328 | As mentioned [above](#), clouds covered the southern Alpine sector on the S2 scenes from August
329 | 2015. Hence, most of the inventory was compiled based on images from [2016](#) and [three](#) scenes
330 | from 2017 ([see Table 1](#)) were used to map glaciers, under clouds or with adverse mapping condi-
331 | tions, i.e. excessive snow cover or shadows in the other scenes. Images acquired in August [2016](#)
332 | had little residual seasonal snow and a high solar elevation at the time of acquisition, which mini-
333 | mised shadow areas creating very good mapping conditions. In September 2016 and October 2017,
334 | more snow was present on high mountain cirques and glacier tongues, but comparatively few snow
335 | patches were found outside glaciers. However, the lower solar elevation compared to August
336 | caused a few north-facing glaciers and glacier accumulation areas to be under shadows. [The raw](#)
337 | [glacier outlines from S2 were corrected by two analysts \(D. Fugazza, R.S. Azzoni\). The outlines](#)
338 | [were separated into regions based on the administrative division of Italy, following the previous](#)
339 | [Italian glacier inventory \(Smiraglia et al. 2015\).](#)

340 |
341 | Seasonal snow and rocks in shadow that were wrongly identified as clean ice were manually delet-
342 | ed by the analysts, as well as lakes and large rivers. In shadow regions, and for glaciers with large
343 | debris cover, the outlines from the previous Italian inventory by Smiraglia et al. (2015) were par-
344 | ticularly valuable as a guide. Where [some small](#) glaciers were entirely under shadows, the outlines
345 | from the previous inventory were copied without changes, while in case of partial shadow cover-
346 | age they were edited in their visible portions. [Due to the comparably small area changes of such](#)
347 | [glaciers over time, the former outlines are likely more precise than a new digitization under such](#)
348 | [conditions \(cf. Fischer et al. 2014\).](#)

349 |
350 | Glaciers in [the Orobic Alps \(ID 12 in Fig. 1\)](#), Dolomites and Julian Alps ([ID 18](#)) posed significant
351 | challenges for [glacier](#) mapping. The three regions host very small niche glaciers and glacierets: in
352 | the Orobic and Julian Alps, their survival is granted by abundant snow-falls, northerly aspect and
353 | accumulation from avalanches, with debris cover also playing an important role. In the Dolomites,
354 | debris cover is often complete (Smiraglia and Diolaiuti 2015), while the steep rock walls provide
355 | shadow and further complicate mapping. For glaciers in the Orobic Alps, an aerial orthophoto ac-
356 | quired by Regione Lombardia ([geoportale.regione.lombardia.it](#)) in 2015 was used to aid the inter-
357 | pretation in view of its finer spatial resolution, (e.g. [Fischer et al. 2014](#), [Leigh et al. 2019](#)), although
358 | the image also shows evidence of seasonal snow. Here, manual delineation of the glacier outlines
359 | was required as the band ratio approach could only detect small snow patches (see Fig. 4c). In the
360 | other two regions, outlines from the previous inventory, derived from aerial orthophotos acquired

fp 28 4 20 3:19 PM
Deleted: important

fp 28 4 20 3:19 PM
Deleted: The raw glacier outlines from S2 were corrected by two analysts (D. Fugazza, R.S. Azzoni). The outlines were separated into regions based on the administrative division of Italy, following the previous Italian glacier inventory (Smiraglia et al. 2015). From west to east, the regions are Aosta Valley, Piemonte, Lombardy, Trento Province, Bolzano Province, Veneto, Friuli, Venezia Giulia. - ... [1]

fp 28 4 20 3:19 PM
Deleted: in the Introduction

fp 28 4 20 3:19 PM
Deleted: August and September

fp 28 4 20 3:19 PM
Deleted: 3

fp 28 4 20 3:19 PM
Deleted: one in August and two in October

fp 28 4 20 3:19 PM
Deleted: also

fp 28 4 20 3:19 PM
Deleted: that were

fp 28 4 20 3:19 PM
Deleted: three sectors of the Alps, i.e.

fp 28 4 20 3:19 PM
Deleted: ,

fp 28 4 20 3:19 PM
Deleted: [2]

fp 28 4 20 3:19 PM
Deleted: ,

383 in 2011, were copied and only corrected where evidence of glacier retreat was found. Whereas the
384 uncertainty in the outlines of the latter glaciers can be large (some of them are marked as 'extinct'
385 in the first Italian inventory from 1959 to 1962), the combined glacier area from the three regions
386 is just above 1% (1.35 km²) of the total area of Italian glaciers. For several of these very small,
387 partly hidden entities one can certainly discuss if they should be kept at all. In this inventory, they
388 have been included for consistency with the last national inventory.

fp 28 4 20 3:19 PM
Deleted: While
fp 28 4 20 3:19 PM
Deleted: these
fp 28 4 20 3:19 PM
Deleted: is likely
fp 28 4 20 3:19 PM
Deleted: ,

389 4.2.4 Switzerland

391 The raw glacier outlines from S2 were corrected by three persons (R. LeBris, F. Paul, P. Rastner)
392 each of them being responsible for a different main region (south of Rhone, north of Rhone/Rhine,
393 south of Rhine). The glacier outlines from the previous inventory by Fischer et al. (2014) were
394 highly valuable for the interpretation, in particular in shadow regions and for glaciers under debris
395 cover. In the hot summer of 2015 most seasonal snow had disappeared by the end of August so
396 that mapping conditions with a comparably high solar elevation (limited regions in shadow) were
397 very good. Some glaciers that could not be identified in the (contrast-stretched) S2 images were
398 either copied from the previous inventory (if located in shadow) or assumed to have disappeared
399 (if sun-lit). Wrongly mapped (turbid) lakes and rivers (Rhone, Aare) were manually removed.

400
401 In a few cases (mostly debris-covered glaciers) we had to deviate from the interpretation of the
402 previous inventories. As shown in Fig. 4d, very high-resolution satellite imagery (as sometimes
403 available in Google Earth) or aerial photography do not always help for a 'correct' interpretation
404 of glacier extents, as the rules applied for identification of ice under debris cover might differ. In
405 this case it seems that the debris-covered region was not corrected in the 2003 and 2008 invento-
406 ries, but is now included (one can still discuss the boundaries). The interpreted glacier area has
407 thus strongly grown since 2003 due to the better visibility of debris cover with S2.

fp 28 4 20 3:19 PM
Deleted: largely
fp 28 4 20 3:19 PM
Deleted: . This
fp 28 4 20 3:19 PM
Deleted: a new interpretation and

408
409 *Figure 4*

411 4.3. Drainage divides and topographic information

412 Drainage divides between glaciers were copied from previous national inventories but were locally
413 adjusted along national boundaries. In part this was required because different DEMs had been
414 used in each country to determine the location of the divide. Additionally, some glaciers are divid-
415 ed by national boundaries rather than flow divides. This can result in an arbitrary part of the glaci-
416 er (e.g. its accumulation zone) being located in one country and the other part (e.g. its ablation
417 zone) in another country. As this makes no sense from a glaciological (and hydrological) point of
418 view, such glaciers (e.g. Hochjochferner in the Ötztal Alps) have been corrected in a way that they
419 belong to the country where the terminus is located. There are thus a few inconsistencies in this
420 inventory compared to the national ones.

421

429 After digital intersection of glacier outlines with drainage divides, topographic information for
430 each glacier entity is calculated from both DEMs (ALOS and TDX) following Paul et al. (2009).
431 The calculation is fully automated and applies the concept of zone statistics introduced by Paul et
432 al. (2002). Each region with a common ID (this includes regenerated glaciers consisting of two
433 polygons) is interpreted as a zone over which statistical information (e.g. minimum / maximum /
434 mean elevation) is derived from an underlying value grid (e.g. a DEM or a DEM-derived slope and
435 aspect grid). Apart from glacier area (in km²) all glaciers have information about mean, median,
436 maximum and minimum elevations, mean slope and aspect (both in degrees) and aspect sector
437 (eight cardinal directions) using letters and numbers (N=1, NE=2, etc.). Further information ap-
438 pended to each glacier in the attribute table of the shape file is the satellite tile used, the acquisition
439 date, the analyst and the funding source. This information is applied automatically by digital inter-
440 section ('*spatial join*') to all glaciers from a manually corrected scene footprint shape file (see Fig.
441 1). The various attributes have then been used for displaying key characteristics of the datasets in
442 bar graphs, scatter plots and maps (see Section 5.1).

444 4.4 Change assessment

445 Glacier area changes have only been calculated with respect to the inventory from 2003, as the
446 dates for the previous national inventories were too diverse for a meaningful assessment (see In-
447 troduction). To obtain consistent changes, only glaciers that are also mapped in the 2003 inventory
448 are used for a direct comparison (automatically selected via a '*point in polygon*' check). However,
449 after realising that a glacier-specific comparison is not possible due to differences in interpretation,
450 (caused by the higher resolution of S2 and the different national rules) and changes in topology
451 (e.g. inclusion of tributaries that were separated in 2003), we decided to only compare the total
452 glacier area of the previous and new inventory.

454 4.5 Uncertainty assessment

455 As several analysts have digitised the new inventory, we decided performing multiple digitising of
456 a pre-selected set of glaciers to determine internal variability in interpretation per participant and
457 across participants as a measure of the uncertainty of the generated dataset. For this purpose, all
458 participants used the same raw outlines from S2 tile 32TLR to manually correct 14 glaciers (sizes
459 from 0.1 to 10 km²) to the south of Lac des Dix around Mt. Blanc de Cheilon (3870 m a.s.l.) for
460 debris cover. All glaciers were digitised 4 times by 5 participants giving a nominal total of 280
461 outlines for comparison. Results were analysed using an overlay of outlines to identify the general
462 deviations in interpretation and through a glacier-by-glacier comparison of glacier sizes. For the
463 latter all datasets were intersected with the same drainage divides and glacier-specific areas were
464 calculated. For each glacier and the entire region, mean area values and standard deviations are
465 calculated per glacier, per participant and for the total sample. The participants were asked to only
466 use the S2 image and the 2003 outlines as a guide for interpretation in the first two digitisation

fp 28 4 20 3:19 PM
Deleted: After
fp 28 4 20 3:19 PM
Deleted: .

469 rounds and consider interpretation of very high-resolution imagery as provided by Google Earth
470 for the second two rounds. At a minimum, one day should have passed between each digitisation
471 round and it was not allowed to show any of the former outlines. On average, each digitisation
472 round took about 2 hours.

473

474 | Additionally, we applied the buffer method (e.g. Paul et al. 2017) to obtain a statistical uncertainty
475 | value for the entire sample. This method gives a minimum and maximum area and was used to
476 | determine a relative area difference. This value multiplied by 0.68 gives the standard deviation
477 | (assuming normally distributed deviations from the correct outline) that is used as a further meas-
478 | ure of area uncertainty (Paul et al. 2017). The selected buffer is based on an earlier multiple digit-
479 | ising experiment for a couple of glaciers (Paul et al. 2013) showing that the variability in the posi-
480 | tioning is within one pixel (or about ± 10 m in the current case) to both sides of the 'true' vector
481 | line. Strictly, a larger buffer should be used for the debris-covered glacier parts, as their uncertain-
482 | ty is higher. However, we have not implemented this here, as the related calculations are computa-
483 | tionally expensive (cf. Mölg et al. 2018) and would still not reflect the real problem in debris iden-
484 | tification as shown in Fig. 4d. Instead, we additionally applied a ± 2 pixels buffer to all glaciers.
485 | For the majority of the debris-covered glaciers (i.e. those where debris can at least be identified)
486 | this gives an upper bound value of the uncertainty. Depending on the degree of debris cover along
487 | the perimeter, the uncertainty is between the two values derived from the two buffers.

488

489 5. Results

490 5.1 The new glacier inventory

491 | In total, we identified 4395 glaciers larger than 0.01 km^2 covering a total area of 1805.88 km^2 , of
492 | which 361.5 km^2 (20%) is found in Austria and 227.1 (12.6%), 325.3 (18%), and 892.1 km^2
493 | (49.4%) in France, Italy, and Switzerland, respectively. The size class distribution by area and
494 | count is depicted in Fig. 5a and also listed in Table 2. In total, 62.5% (92%) of all glaciers are
495 | smaller than 0.1 km^2 (1.0 km^2) covering 5.5% (28%) of the glacierised area, whereas 1.6% are
496 | larger than 5 km^2 and cover 40%. Thereby, glaciers in the size class 1 to 5 km^2 alone cover one
497 | third (31.5%) of the area but only 6.4% of the total number. This biased size class distribution is
498 | typical for alpine glaciers where a few large glaciers are surrounded by numerous much smaller
499 | ones. The distribution of glacier number and area by aspect sector displayed in Fig. 5b shows the
500 | dominance, both in number and coverage area, of northerly exposed glaciers compared to all other
501 | sectors. About 60% of all glaciers (covering 60% of the area) are exposed to the NW, N, or NE
502 | whereas only 21% of all glaciers are found in the sectors SE, S, and SW. This distribution of glaci-
503 | er aspects is typical for regions where radiation plays a larger role in glacier existence compared to
504 | factors such as precipitation (Evans and Cox, 2005). The larger area coverage for glaciers facing
505 | SE is mostly due to the large Aletsch and Fiescher glaciers.

- fp 28 4 20 3:19 PM
Deleted:)
- fp 28 4 20 3:19 PM
Deleted: also
- fp 28 4 20 3:19 PM
Deleted: coverage, a realistic
- fp 28 4 20 3:19 PM
Deleted: estimate
- fp 28 4 20 3:19 PM
Deleted: likely
- fp 28 4 20 3:19 PM
Deleted: these
- fp 28 4 20 3:19 PM
Deleted: 4394
- fp 28 4 20 3:19 PM
Deleted: 77
- fp 28 4 20 3:19 PM
Deleted: 0
- fp 28 4 20 3:19 PM
Deleted: 63
- fp 28 4 20 3:19 PM
Deleted: 32

517
518
519
520
521
522
523
524
525
526
527
528
529
530
531
532
533
534
535
536
537
538
539
540
541
542
543
544
545
546
547
548
549
550
551
552
553
554
555
556
557

Figure 5, Table 2

A plot of glacier surface area vs. minimum and maximum elevations (Fig. 6a) reveals that glaciers smaller than 1 km² cover nearly the full range of possible elevations, indicating that their mean elevation is also impacted by factors other than climate (i.e. they can also exist at low elevations when they are located in a well protected environment). Glaciers larger than 1 km² on the other hand have clearly distinguished maximum and minimum elevations, *i.e.* they arrange around a climatically driven mean elevation which is around 3000 m a.s.l. Plotting glacier area vs. elevation range (Fig. 6b) shows that the largest glaciers are not those with the highest elevation range (the maximum of 3140 m is for Glacier des Bossons in the Mont-Blanc massif with a size of 10 km²) and that for the majority of glaciers the elevation range increases with glacier size. This is typical for regions dominated by mountain and valley glaciers as these follow the given topography. The ca. 7 km² large Plaine Morte Glacier is a plateau glacier with an elevation range of only 350 m and represents an exception from the rule that larger glaciers have generally a larger elevation range.

Figure 6

The median elevation of a glacier is largely driven by temperature, precipitation and radiation, receipt (that depends on topography). As temperature is rather similar at the same elevation over large regions (*e.g.* Zemp et al. 2007) and topography (aspect / shading) has a strong local impact on radiation receipt, the large-scale variability of median (or mean) elevation of a glacier has a high correlation with precipitation (*e.g.* Ohmura et al. 1992, Oerlemans 2005, Rastner et al. 2012, Sakai et al. 2015). The spatial distribution of glacier median elevations in the Alps (Fig. 7) thus also reflects the general pattern of annual precipitation amounts (*e.g.* Frei et al. 2003). When focusing on glaciers larger than 0.5 km² (that are less impacted by local topographic conditions), clearly lower median elevations (around 2400 m a.s.l.) are found for glaciers along the northern margin of the Alps and major mountain passes than in the inner Alpine valleys (around 3700 m a.s.l.) that are well shielded from precipitation. On top of this variability comes the variability due to a different aspect (Fig. 7, inset): On average, glaciers that are exposed to the south have median elevations that are about 250 m higher (mean 3125 m a.s.l.) than north-facing glaciers (mean 2875 m a.s.l.). However, the scatter is high and for each aspect the elevation variability is about 1500 m.

Figure 7

The graph in Fig. 8 shows the hypsometry of glacier area in the four countries and for the total area in relative terms. On average, the highest area share is found around the mean elevation of 3000 m a.s.l. By referring for each country to the total area as 100%, differences among them can be seen. Most notable is the smaller elevation range and larger peak of glaciers in Austria, the broader vertical distribution in Switzerland (with the lowest peak value), and the slightly higher peak of the distribution in Italy (at 3100 m a.s.l.). The hypsometry of glaciers in France is closest to the curve

fp 28 4 20 3:19 PM
Deleted: can be found at all
fp 28 4 20 3:19 PM
Deleted: does only slightly depend on climatic
fp 28 4 20 3:19 PM
Deleted: .

fp 28 4 20 3:19 PM
Deleted: .

fp 28 4 20 3:19 PM
Deleted: amounts
fp 28 4 20 3:19 PM
Deleted: 7a

fp 28 4 20 3:19 PM
Deleted: 7b
fp 28 4 20 3:19 PM
Deleted: 400
fp 28 4 20 3:19 PM
Deleted: at 3200
fp 28 4 20 3:19 PM
Deleted: at 2800

569 for the entire Alps.

570
571
572
573

Figure 8

5.2 Area changes

574 For a selection of 2873 [comparable polygon entities](#) present in both inventories, total glacier area
575 shrunk from 2060 km² in 2003 to 1783 km² in 2015/16 or by -13.2% (-1.1%/a). Considering the
576 assumed missing area in the 2003 inventory of about 40 km² (glaciers with area gain are 29.4 km²
577 larger in 2015/16 than in 2003), a more realistic area loss is -15% or -1.3%/a. This is about the
578 same pace as reported earlier by Paul et al. (2004) for the Swiss Alps from 1985 to 1998/99 (-
579 1.4%/a). An example of the strong glacier shrinkage in Austria is depicted in Fig. 9. Closer inspec-
580 tion of this image also reveals [a small shift \(to the SE\) of the S2 scenes compared to the earlier](#)
581 Landsat TM scenes.

582
583
584

Figure 9

585 The comparison of glacier outlines in Fig. 10 illustrate for the region around Sonnblickkees in
586 Austria why we do not provide a scatterplot of relative area changes vs. glacier size or country
587 specific area change values (cf. also Fig. 4d for Gavirolas Glacier in Switzerland). Due to the dif-
588 ferent interpretations in the new inventory, 125 mostly very small glaciers are 100% to 630% larg-
589 er than in 2003 and a large number (557) is 0% to 100% larger. For example, the 4 km² Suldenfer-
590 ner has increased in size by 550% as a small tributary (that holds the ID for the glacier) was dis-
591 connected in 2003 but is now connected to the entire glacier. Although such cases can be manually
592 adjusted, it would not solve the general problem of the different interpretation [when using data](#)
593 [sources with differing spatial resolution \(cf. Fischer et al. 2014, Leigh et al. 2019\)](#). For example,
594 the glacier in Fig. 4d has increased its size from 2003 to 2015 by 56% due to the new interpreta-
595 tion. On the other hand, Careser glacier, which fragmented in six ice bodies from 2003 to 2015,
596 lost 55% of its area when summing up all parts as opposed to 63% when considering the largest
597 glacier only. In consequence, the possible area reduction due to melting is partly compensated by
598 the more generous interpretation of glacier extents and thus with a limited meaning on the basis of
599 individual glaciers. [Overall, glacier extents in the 2015/16 inventory might be somewhat larger](#)
600 [than in reality due to the inclusion of seasonal/perennial snow in some regions. The -15% area loss](#)
601 [mentioned above can thus be seen as a lower bound estimate.](#)

602
603
604

Figure 10

5.3 Uncertainties

5.3.1 Glacier outlines

606 The multiple digitising experiment revealed several interesting albeit well-known results. Overall,
607 the area uncertainty (one standard deviation, STD) is 3.3% across all participants for the total of
608

fp 28 4 20 3:19 PM
Deleted: glaciers

fp 28 4 20 3:19 PM
Deleted: the

fp 28 4 20 3:19 PM
Deleted: .

fp 28 4 20 3:19 PM
Deleted: Assuming that some glaciers

fp 28 4 20 3:19 PM
Deleted: are

fp 28 4 20 3:19 PM
Deleted: included

fp 28 4 20 3:19 PM
Deleted: , the real

fp 28 4 20 3:19 PM
Deleted: would be even higher than the pre-
viously estimated -15%.

618 the digitised area (Table 3). As two glaciers (11 and 13) were not mapped by one participant, the
 619 missing values are replaced with the mean value from the other participants. Across all glaciers but
 620 for individual participants the uncertainty (comparing the values from the four digitisation rounds)
 621 is considerably lower (1% to 2.7%), indicating that the digitising is more consistent when per-
 622 formed by the same person. The area values of participant 1 (P1) are systematically higher than for
 623 the other participants, about 6% for the total area. A detailed analysis ([close-ups and only showing](#)
 624 [individual datasets](#)) of the digitised outlines (Fig. 11) revealed that the differences are mostly due
 625 to the more generous inclusion of debris-covered glacier ice for two of the larger glaciers (Nr. 1
 626 and 5). When excluding P1, the STD across the other participants is three times smaller (1.1%).
 627 The uncertainty also slightly depends on glacier size, showing values between 1% and 6% for
 628 glaciers larger than 1 km² and between 2% and 20% for glacier <1 km². The smallest glacier in the
 629 sample is smaller than 0.1 km² and shows variations in STD between 8% and 44%, in the latter
 630 case also due to a reinterpretation of its extent when using very high-resolution imagery. For such
 631 small glaciers related changes can thus result in considerably different extents.

632
 633 *Table 3, Figure 11*

634 Moreover, for P1 and most of the other participants the digitised glacier extents increased by sev-
 635 eral per cent after consultation of very high-resolution satellite images as available in Google Earth
 636 and [from the swisstopo map server](#) ([Supplement, Fig. S1](#)). The generally very flat and debris-
 637 covered regions were barely visible on the S2 images and have been digitised differently in each of
 638 the four rounds. Hence, the possibility for a re-interpretation of the outlines within the same exper-
 639 iment resulted in higher standard deviations. If such regions have to be included in a glacier inven-
 640 tory or not can be discussed, as the transition to ice-cored medial or lateral moraines is often grad-
 641 ual and including these features in a glacier inventory or not is a (personal) methodological deci-
 642 sion. [The Figs. S2 and S3 in the Supplement provide examples of the difficulties in interpreting](#)
 643 [such regions. Even at this high spatial resolution the exact boundary of the two glaciers is not fully](#)
 644 [clear so that a large interpretation spread can be expected at lower resolution. However, in general](#)
 645 [it seems that the area of glaciers with debris-covered margins is still slightly underestimated at 10](#)
 646 [m resolution. This](#) confirms earlier recommendations to double-check all digitised glacier extents
 647 with such very high-resolution sensors, at least for [the difficult cases](#) (e.g. Fischer et al. 2014).

648
 649 The uncertainty (one STD) obtained with the buffer method is $\pm 5\%$ (10%) when using a 10 m (20
 650 m) buffer. [Considering that the former buffer might be a realistic uncertainty bound for clean ice](#)
 651 [and the latter for debris-covered ice, the ‘true’ uncertainty value would be between 5 and 10% and](#)
 652 [for individual glaciers largely depend on the difficulties in identifying ice under debris.](#) This is in
 653 line with the [uncertainties derived from the multiple digitising](#) and numerous previous studies.

654
 655
 656 **5.3.2 Topographic information**

fp 28 4 20 3:19 PM
 Deleted: the aerial imagery

fp 28 4 20 3:19 PM
 Deleted: .

fp 28 4 20 3:19 PM
 Deleted: very

fp 28 4 20 3:19 PM
 Deleted: However, it points to an underesti-
 mation of glacier area also with 10 m resolu-
 tion sensors and

fp 28 4 20 3:19 PM
 Deleted: ‘difficult’ glaciers

fp 28 4 20 3:19 PM
 Deleted: mean values of the

fp 28 4 20 3:19 PM
 Deleted: experiment

666 The comparison of [topographic parameters](#) (minimum, maximum and mean elevation, mean slope
 667 and aspect) [as](#) derived from the TDX and AW3D30 DEM, revealed [larger differences](#), in particular
 668 towards smaller glaciers. [These](#) are more likely to be impacted by [artifacts](#) as [they](#) share a [larger](#)
 669 percentage of their total area. [\(see Fig. 2\)](#). Differences in mean slope and aspect are generally small
 670 but increase towards larger slope values for the former. This is in agreement with the general ob-
 671 servations that DEM quality is reduced at steep slopes. Minimum elevation is slightly higher in the
 672 TDX DEM, which can be explained by glacier retreat between the acquisition dates, [\(around 2009](#)
 673 [for AW3D30 vs. around 2013 for TDX\)](#). However, a clearly lower mean elevation due an overall
 674 surface lowering of the glaciers could not be observed, indicating that the differences are in the
 675 uncertainty range. Apart from artefacts, the uncorrected radar penetration of the TDX DEM might
 676 play a role here as well.

678 6. Discussion

679 The derived size class distribution (Fig. 5) and topographic information are typical for glaciers in
 680 mid-latitude mountain ranges with numerous smaller glaciers surrounding a few larger ones. [\(e.g.](#)
 681 [Pfeffer et al. 2014\)](#). Only [349](#) out of [4395](#) glaciers (8%) are larger than 1 km² and nearly one half
 682 (46%) is smaller than 0.05 km² covering 2.7% of the area. It might be well possible that many of
 683 the latter are no longer glaciers but just perennial snow and firn patches. However, for consistency
 684 with earlier [national glacier](#) inventories they have been included. Mean elevation values do not
 685 really depend on [size](#) for such [‘glaciers’](#), indicating that they can survive at different elevations
 686 and precipitation amounts have a limited impact, [on their occurrence \(e.g. if fed by avalanche](#)
 687 [snow\)](#). If they are well protected from solar radiation (e.g. by shadow or debris cover) such glaci-
 688 ers might persist for some time despite increasing air temperatures. Glacier mean elevation [does](#)
 689 not depend on glacier size but [on](#) glacier location with respect to precipitation sources, in particu-
 690 lar for larger glaciers (Fig. 7). [On top of this dependence is the variability with mean aspect \(Fig.](#)
 691 [7, inset\)](#).

693 Widespread glacier thinning [over the past decades](#) and steep terrain resulted lately in interrupted
 694 profiles for several larger valley glaciers. [Their](#) lower parts are [now](#) no longer nourished by ice
 695 from above. [These separated](#) parts [can thus](#) not be named [‘regenerated glaciers’](#) but [they](#) melt
 696 away as dead ice. Strictly speaking, such lower dead ice bodies (that can persist due to debris cov-
 697 er for a very long time) should be excluded from a glacier inventory (Raup and Khalsa 2007).
 698 However, for consistency with former inventories and their contribution to run-off we included
 699 them here and [used the same ID for both parts](#) to obtain [topographic information](#) for the combined
 700 extent. Calculating this instead for the individual parts would result in related outliers and a more
 701 difficult analysis of trends. At best, such separated parts are identified with a flag in the attribute
 702 table, for example as a further extension to the ‘Form’ attribute (e.g. ‘4: Separated glacier part’)
 703 used in the RGI (RGI consortium 2017). However, the differentiation from a regenerated glacier

- fp 28 4 20 3:19 PM
Deleted: glacier
- fp 28 4 20 3:19 PM
Deleted: as well as
- fp 28 4 20 3:19 PM
Deleted: ,
- fp 28 4 20 3:19 PM
Deleted: larger differences. Smaller glaciers
- fp 28 4 20 3:19 PM
Deleted: artefacts
- fp 28 4 20 3:19 PM
Deleted: these easily
- fp 28 4 20 3:19 PM
Deleted: large
- fp 28 4 20 3:19 PM
Deleted: .
- fp 28 4 20 3:19 PM
Deleted: .
- fp 28 4 20 3:19 PM
Deleted: .
- fp 28 4 20 3:19 PM
Deleted: .
- fp 28 4 20 3:19 PM
Deleted: 354
- fp 28 4 20 3:19 PM
Deleted: 4394
- fp 28 4 20 3:19 PM
Deleted: glacier
- fp 28 4 20 3:19 PM
Deleted: glaciers
- fp 28 4 20 3:19 PM
Deleted: .
- fp 28 4 20 3:19 PM
Deleted: (about 3000 m a.s.l.)
- fp 28 4 20 3:19 PM
Deleted: is modified by
- fp 28 4 20 3:19 PM
Deleted: and mean aspect
- fp 28 4 20 3:19 PM
Deleted: whose
- fp 28 4 20 3:19 PM
Deleted: In other words, these
- fp 28 4 20 3:19 PM
Deleted: are
- fp 28 4 20 3:19 PM
Deleted: glaciers
- fp 28 4 20 3:19 PM
Deleted: merged their IDs
- fp 28 4 20 3:19 PM
Deleted: more reasonable

728 might sometimes be difficult.

729

730 Due to the differences in interpretation (Fig. 10) we have not compared the 2003 extents of indi-
731 vidual glaciers directly with those from the new inventory but only the total area of glaciers ob-
732 served in both inventories. Considering the underestimated glacier area in 2003 (e.g. due to miss-
733 ing debris cover) and possibly overestimated sizes in 2015 (e.g. due to included snow) the pace of
734 shrinkage (-1.3% /a) has not changed compared to the earlier mid-1980s to 2003 period. This indi-
735 cates that most glaciers have not yet reached a geometry that is compliant with current climate
736 conditions and will thus continue shrinking in the future. This becomes also clear from the snow
737 cover remaining near the end of the ablation period on the glaciers, covering barely 20% to 30% of
738 the area (e.g. Figs. 9 and 11). Assuming a required 60% coverage of their accumulation area, glac-
739 iers in the Alps have to lose another 50% to 70% of their area to reach again balanced mass budg-
740 ets (Carturan et al. 2013). There are other regions in the world with similar high (or even higher)
741 area loss rates such as the tropical Andes (e.g. Rabatel et al. 2013), but to a large extent this is also
742 due to the smaller glaciers in this region. A realistic comparison across regions would only be pos-
743 sible when change rates of identical size classes are compared.

744

745 The multiple digitising experiment (Fig. 11) revealed a large variability in the interpretation of de-
746bris-covered glaciers among the analysts but high consistency in the corrections where boundaries
747 are well visible. Related area uncertainties can be high for very small glaciers (>20%) but are gen-
748 erally <5%. The here derived area reduction of about -15% since 2003 is thus significant, but for
749 small and/or debris-covered glaciers the area uncertainty can be similar to the change, making it
750 less reliable. However, this strongly depends on the specific glacier characteristics and cannot be
751 generalized to all small glaciers.

752

753 The gradual disappearance of ice under debris cover and the separation of low-lying glacier
754 tongues on steep slopes are major problems for any glacier inventory created these days. We de-
755 cided to re-connect disconnected glacier parts by their ID (to so-called *multi-part polygons*) for
756 consistency with earlier inventories. However, keeping them separated is another possibility, given
757 that possible dead ice is clearly marked in the attribute table.

758

759 7. Conclusions

760 We presented the results of a new glacier inventory for the entire Alps derived from Sentinel-2
761 images of 2015 and 2016. In total, [4395](#) glaciers >0.01 km² covering an area of 1806 ±60 km² are
762 mapped. This is a reduction of about 300 km² or -15% (-1.3%/a) compared to the previous Alpine-
763 wide inventory from 2003. The pace of glacier shrinkage in the Alps remained about the same
764 since the mid-1980's, indicating that glaciers will continue to shrink under current climatic condi-
765 tions. Due to the differences in interpretation, we have not performed a glacier-by-glacier compari-

767 son of area changes. The on-going glacier decline also results in increasingly difficult glacier iden-
768 tification (under debris cover) and topologic challenges for a database (when glaciers split). The
769 former is confirmed by the results of the uncertainty assessment, showing a large variability in the
770 interpretation of glacier extents when conditions are challenging. Despite the additional workload,
771 we think this is the best way to provide an uncertainty value for such a highly corrected and
772 merged dataset. In any case, the outlines from the new inventory should be more accurate than for
773 2003, as we here used the previous, high-quality national inventories as a guide for interpretation,
774 performed corrections by the respective experts, and worked with the higher resolution of Senti-
775 nel-2 data that helped in identifying important spatial details.

776
777 The clean-ice mapping with the band ratio method is straightforward, but requires well-thought
778 decisions on the two thresholds as they will always be a compromise. They should be tested in re-
779 gions with ice in cast shadow and selected in a way that the workload for manual corrections is
780 minimised. If a precise DEM is available, the required corrections of wrongly mapped ice in shad-
781 ow can be reduced as the further pre-processing for glaciers in Austria revealed. However, reduced
782 DEM quality and illumination differences can limit the benefits of a topographic normalisation of
783 the images. Due to the artefacts in the first version of the TanDEM-X DEM, we used the ALOS
784 AW3D30 DEM to derive topographic information for each glacier despite the less good temporal
785 agreement. To conclude, we had datasets [with a much higher spatial resolution](#) available for this
786 inventory compared to the 2003 dataset, but for several reasons (e.g. debris cover, clouds, seasonal
787 snow) the creation of glacier inventories from satellite data and a DEM remains a challenging task
788 with high workload and expert knowledge required.

789

790 8. Data availability

791 The dataset can be downloaded from: <https://doi.pangaea.de/10.1594/PANGAEA.909133> (Paul et
792 al., 2019).

793

794 Author contributions

795 FP designed the study, prepared raw glacier outlines, performed various calculations and wrote the
796 draft manuscript. PR performed most of the GIS-based calculations and the editing that was re-
797 quired to obtain a complete dataset and change assessment (e.g. DEM mosaicking, dataset merg-
798 ing, [drainage divides](#), topographic [attributes](#), [satellite footprints](#)). All authors processed, corrected
799 and checked the created glacier outlines in their country and contributed to the contents and editing
800 of the manuscript. FP, DF, JN, AR, and PR performed the multiple digitising of glacier outlines for
801 uncertainty assessment.

802

fp 28 4 20 3:19 PM
Deleted: co-registration issues as well as local

fp 28 4 20 3:19 PM
Deleted: much better

fp 28 4 20 3:19 PM
Deleted: <https://doi.pangaea.de/10.1594/PANGAEA.909133>

fp 28 4 20 3:19 PM
Deleted: the

fp 28 4 20 3:19 PM
Deleted: drainage divides, satellite footprints, country boundaries,

fp 28 4 20 3:19 PM
Deleted: and co-registration

fp 28 4 20 3:19 PM
Deleted: data

813 **Competing interest**

814 The authors declare that they have no conflict of interests.

815

816 **Acknowledgements**

817 This study has been performed in the framework of the project Glaciers_cci (4000109873/14/I-
818 NB) and the Copernicus Climate Change Service (C3S) that is funded by the European Union and
819 implemented by ECMWF. R.S. Azzoni and D.Fugazza were funded by DARA - Department for
820 regional affairs and autonomies of the Italian presidency of the council of Ministers (funding code
821 COLL_MIN15GDIOL_M) and Levissima Sanpellegrino S.P.A., (funding code
822 LIB_VT17GDIOL). For the French Alps contribution, A. Rabatel and M. Ramusovic acknowledge
823 the *Service National d'Observation* GLACIOCLIM (Univ. Grenoble Alpes, CNRS, IRD, IPEV,
824 <https://glacioclim.osug.fr/>), the LabEx OSUG@2020 (*Investissements d'avenir* – ANR10
825 LABX56), the EquipEx GEOSUD (*Investissements d'avenir* – ANR-10-EQPX-20), the CNES /
826 Kalideos Alpes and CNES / SPOT-Image ISIS program #2011-513 for providing the Pléiades im-
827 ages and SPOTDEM from 2011, and J.P. Dedieu for its involvement in the glaciological invento-
828 ries of the French Alps during past decades. For the Austrian Alps, G. Schwaizer and J. Nemeč
829 acknowledge funding from the Environmental Earth Observation (ENVEO) IT GmbH and the
830 Austrian Research Promotion Agency (FFG) within the ASAP9-SenSAP project (3574408). The
831 AW3D30 DEM is provided by the Japan Aerospace Exploration Agency ([http://www.eorc.](http://www.eorc.jaxa.jp/ALOS/en/aw3d30/index.htm)
832 [jaxa.jp/ALOS/en/aw3d30/index.htm](http://www.eorc.jaxa.jp/ALOS/en/aw3d30/index.htm)) ©JAXA. Figures 3, 4, 9, 10, and 11 contain modified Coper-
833 nicus Sentinel data (2015, 2016). We would also like to thank A. Fischer and S. Herreid for their
834 constructive comments that helped considerably in improving the clarity of the paper.

835

fp 28 4 20 3:19 PM
Deleted: .

- 838 [Auer, I., Böhm, R., Jurkovic, A., Lipa, W., Orlik, A., Potzmann, R., Schöner, W., Ungersböck, M.,](#)
839 [Matulla, C., Briffa, K., Jones, P.D., Efthymiadis, D., Brunetti, M., Nanni, T., Maugeri, M.,](#)
840 [Mercalli, L., Mestre, O., Moisselin, J.-M., Begert, M., Müller-Westermeier, G., Kveton, V.,](#)
841 [Bochnicek, O., Stastny, P., Lapin, M., Szalai, S., Szentimrey, T., Cegnar, T., Dolinar, M.,](#)
842 [Gajic-Capka, M., Zaninovic, K., Majstorovic, Z. and Nieplova, E.: HISTALP – historical in-](#)
843 [strumental climatological surface time series of the greater Alpine region 1760-2003, *Internat-*](#)
844 [ional Journal of Climatology](#), 27, 17-46, 2007.
- 845 Beniston, M., Diaz, H.F., and Bradley, R.S.: Climatic change at high elevation sites: A review,
846 *Climatic Change*, 36, 233-251, 1997.
- 847 Böhm, R., Auer, I., Brunetti, M., Maugeri, M., Nanni, T., and Schöner, W.: Regional temperature
848 variability in the European Alps 1760–1998 from homogenized instrumental time series, *Internat-*
849 *ional Journal of Climatology*, 21, 1779-1801, 2001.
- 850 Carturan, L., Filippi, R., Seppi, R., Gabrielli, P., Notarnicola, C., Bertoldi, L., Paul, F., Rastner, P.,
851 Cazorzi, F., Dinale, R., and Dalla Fontana, G.: Area and volume loss of the glaciers in the Ort-
852 les-Cevedale group (Eastern Italian Alps): Controls and imbalance of the remaining glaciers,
853 *The Cryosphere*, 7, 1339-1359, 2013.
- 854 Casty, C., Wanner, H., Luterbacher, J., Esper, J., and Böhm, R.: Temperature and precipitation
855 variability in the European Alps since 1500, *International Journal of Climatology*, 25 (14),
856 1855-1880, 2005.
- 857 Dozier, J.: Spectral signature of alpine snow cover from Landsat 5 TM, *Remote Sensing of Envi-*
858 *ronment*, 28, 9-22, 1989.
- 859 Evans, I.S., and Cox, N.J.: Global variations of local asymmetry in glacier altitude: Separation of
860 north-south and east- west components, *Journal of Glaciology*, 51 (174), 469-482, 2005.
- 861 Fischer, M., Huss, M., Barboux, C., and Hoelzle, M.: The new Swiss Glacier Inventory SGI2010:
862 Relevance of using high-resolution source data in areas dominated by very small glaciers, *Arctic,*
863 *Antarctic and Alpine Research*, 46(4), 933-945, 2014.
- 864 Fischer, A., Seiser, B., Stocker-Waldhuber, M., Mitterer, C., and Abermann, J.: Tracing glacier
865 changes in Austria from the Little Ice Age to the present using a lidar-based high-resolution
866 glacier inventory in Austria, *The Cryosphere*, 9, 753-766, 2015.
- 867 Frei, C.: Interpolation of temperature in a mountainous region using nonlinear profiles and non-
868 Euclidean distances, *International Journal of Climatology*, 34, 1585-1605, 2014.
- 869 Frei, C., Christensen, J.H., Déqué, M., Jacob, D., Jones, R.G., and Vidale, P.L.: Daily precipitation
870 statistics in regional climate models: Evaluation and intercomparison for the European Alps,
871 *Journal of Geophysical Research*, 108(D3), 4124, doi: 10.1029/2002JD002287, 2003.
- 872 Gardent, M., Rabatel, A., Dedieu, J.-P., and Deline, P.: Multitemporal glacier inventory of the
873 French Alps from the late 1960s to the late 2000s, *Global and Planetary Change*, 120, 24-37,
874 2014.
- 875 Gardner, A. S., Moholdt, G., Cogley, J. G., Wouters, B., Arendt, A. A., Wahr, J., Berthier, E.,
876 Hock, R., Pfeffer, W. T., Kaser, G., Ligtenberg, S. R. M., Bolch, T., Sharp, M. J., Hagen, J. O.,
877 van den Broeke, M. R., and Paul, F.: A consensus estimate of glacier contributions to sea level
878 rise: 2003 to 2009, *Science*, 340 (6134), 852-857, 2013.
- 879 Kääb, A., Winsvold, S.H., Altena, B., Nuth, C., Nagler, T., and Wuite, J.: Glacier remote sensing
880 using Sentinel-2. Part I: Radiometric and geometric performance, and application to ice veloci-
881 ty, *Remote Sensing*, 8, 598, doi:10.3390/rs8070598, 2016.
- 882 Kienholz, C., Hock, R., and Arendt, A.A.: A new semi-automatic approach for dividing glacier
883 complexes into individual glaciers, *Journal of Glaciology*, 59 (217), 925-936, 2013.

884 Lambrecht, A., and Kuhn, M. (2007): Glacier changes in the Austrian Alps during the last three
885 decades, derived from the new Austrian glacier inventory, *Annals of Glaciology* 46, 177-184,
886 2007.

887 [Leigh, J.R., Stokes, C.R., Carr, R.J., Evans, I.S., Andreassen, L.M., and Evans, D.J.A.: Identifying
888 and mapping very small \(<0.5 km²\) mountain glaciers on coarse to high-resolution imagery,
889 *Journal of Glaciology*, 65\(254\), 873-888, 2019.](#)

890 Marzeion, B., Champollion, N., Haeberli, W., Langley, K., Leclercq, P., and Paul, F.: Observation
891 of glacier mass changes on the global scale and its contribution to sea level change, *Surveys in
892 Geophysics*, 38 (1), 105-130, 2017.

893 Mölg, N., Bolch, T., Rastner, P., Strozzi, T., and Paul, F.: A consistent glacier inventory for the
894 Karakoram and Pamir region derived from Landsat data: Distribution of debris cover and
895 mapping challenges, *Earth Systems Science Data*, 10, 1807-1827, 2018.

896 Mölg, N., Bolch, T., Walter, A., and Vieli, A.: Unravelling the evolution of Zmuttgletscher and its
897 debris cover since the end of the Little Ice Age, *The Cryosphere*, 13, 1889-1909, 2019.

898 Oerlemans, J.: Extracting a climate signal from 169 glacier records, *Science*, 308, 675- 677, 2005.

899 Ohmura, A., Kasser, P., and Funk, M.: Climate at the equilibrium line of glaciers, *Journal of Glac-*
900 *iology*, 38(130), 397-411, 1992.

901 Paul, F., Kääb, A., Maisch, M., Kellenberger, T.W., and Haeberli, W.: The new remote-sensing-
902 derived Swiss glacier inventory: I. Methods, *Annals of Glaciology*, 34, 355-361, 2002.

903 Paul, F., Kääb, A., Maisch, M., Kellenberger, T.W., and Haeberli, W.: Rapid disintegration of Al-
904 pine glaciers observed with satellite data, *Geophysical Research Letters*, 31, L21402, doi:
905 10.1029/2004GL020816, 2004.

906 Paul, F., Barry, R., Cogley, J.G., Frey, H., Haeberli, W., Ohmura, A., Ommanney, C.S.L, Raup,
907 B., Rivera, A., and Zemp, M.: Recommendations for the compilation of glacier inventory data
908 from digital sources, *Annals of Glaciology*, 50 (53), 119-126, 2009.

909 Paul, F., Frey, H., and Le Bris, R.: A new glacier inventory for the European Alps from Landsat
910 TM scenes of 2003: Challenges and results, *Annals of Glaciology*, 52 (59), 144-152, 2011.

911 Paul, F., Barrand, N. E., Baumann, S., Berthier, E., Bolch, T., Casey, K., Frey, H., Joshi, S. P.,
912 Kononov, V., Le Bris, R., Mölg, N., Nosenko, G., Nuth, C., Pope, A., Racoviteanu, A.,
913 Rastner, P., Raup, B., Scharrer, K., Steffen, S., and Winsvold, S.H.: On the accuracy of glacier
914 outlines derived from remote sensing data, *Annals of Glaciology*, 54 (63), 171-182, 2013.

915 Paul, F., Winsvold, S.H., Kääb, A., Nagler, T., and Schwaizer, G.: Glacier remote sensing using
916 Sentinel-2. Part II: Mapping glacier extents and surface facies, and comparison to Landsat 8.
917 *Remote Sensing*, 8(7), 575; doi:10.3390/rs8070575, 2016.

918 Paul, F., Bolch, T., Briggs, K., Kääb, A., McMillan, M., McNabb, R., Nagler, T., Nuth, C.,
919 Rastner, P., Strozzi, T., and Wuite, J.: Error sources and guidelines for quality assessment of
920 glacier area, elevation change, and velocity products derived from satellite data in the Glaci-
921 ers_cci project, *Remote Sensing of Environment*, 203, 256-275, 2017.

922 Paul, F., Rastner, P., Azzoni, R.S., Diolaiuti, G., Fugazza, D., Le Bris, R., Nemeč, J., Rabatel, A.,
923 Ramusovic, M., Schwaizer, G., and Smiraglia, C.: Glacier inventory for the Alps, online:
924 <https://doi.pangaea.de/10.1594/PANGAEA.909133>, 2019.

925 Pfeffer, W. T., Arendt, A.A., Bliss, A., Bolch, T., Cogley, J. G., Gardner, A. S., Hagen, J.-O.,
926 Hock, R., Kaser, G., Kienholz, C., Miles, E.S., Moholdt, G., Mölg, N., Paul, F., Radic, V.,
927 Rastner, P., Raup, B.H., Rich, J., Sharp, M.J., and the Randolph Consortium: The Randolph
928 Glacier Inventory: A globally complete inventory of glaciers, *Journal of Glaciology*, 60 (221),
929 537-552, 2014.

930 Rabatel, A., and 27 others: Current state of glaciers in the tropical Andes: a multi-century perspec-
931 tive on glacier evolution and climate change, *The Cryosphere*, 7, 81-102, 2013.

932 Rabatel, A., Ceballos, J.L., Micheletti, N., Jordan, E., Braitmeier, M., Gonzales, J., Moelg, N.,
933 Ménégoz, M., Huggel, C., and Zemp, M.: Toward an imminent extinction of Colombian glaciers?
934 *Geografiska Annaler: Series A, Physical Geography*, 100 (1), 75-95, 2018.

935 Racoviteanu, A.E., Paul, F., Raup, B., Khalsa, S.J.S., and Armstrong, R.: Challenges in glacier
936 mapping from space: Recommendations from the Global Land Ice Measurements from Space
937 (GLIMS) initiative, *Annals of Glaciology*, 50 (53), 53-69, 2009.

938 Rastner, P., Bolch, T., Mölg, N., Machguth, H., Le Bris, R., and Paul, F.: The first complete inven-
939 tory of the local glaciers and ice caps on Greenland, *The Cryosphere*, 6, 1483-1495, 2012.

940 Raup, B., and Khalsa, S.J.S.: GLIMS Analysis Tutorial, 15 pp. Online at:
941 <http://www.glims.org/MapsAndDocs/guides.html>, 2007.

942 Reid, P. C., Hari, R.E., Beaugrand, G., Livingstone, D.M., Marty, C., Straile, D., Barichivich, J.,
943 Goberville, E., Adrian, R., Aono, Y., Brown, R., Foster, J., Groisman, P., Hélaouët, P., Hsu,
944 H., Kirby, R., Knight, J., Kraberg, A., Li, J., Lo, T., Myneni, R.B., North, R.P., Pounds, J.A.,
945 Sparks, T., Stübi, R., Tian, Y., Wiltshire, K.H., Xiao, D., and Zhu, Z.: Global impacts of the
946 1980s regime shift, *Global Change Biology*, 22(2), 682-703, 2016.

947 RGI consortium: Randolph Glacier Inventory – A Dataset of Global Glacier Outlines: Version 6.0,
948 GLIMS Technical Report, 71 pp., online at: glims.org/RGI/00_rgi60_TechnicalNote.pdf,
949 2017.

950 Sakai, A., Nuimura, T., Fujita, K., Takenaka, S., Nagai, H., and Lamsal, D. (2015): Climate re-
951 gime of Asian glaciers revealed by GAMDAM glacier inventory, *The Cryosphere*, 9, 865-880.

952 Smiraglia, C., Diolaiuti, G.A.: The new Italian glacier inventory, 1st ed., Ev-K2-CNR Publica-
953 tions, Bergamo, 2015.

954 Smiraglia, P., Azzoni, R.S., D'Agata, C., Maragno, D., Fugazza, D., and Diolaiuti, G.A.: The evo-
955 lution of the Italian glaciers from the previous data base to the new Italian inventory. Prelimi-
956 nary considerations and results, *Geografia Fisica e Dinamica Quaternaria* 38, 79-87, 2015.

957 Stumpf, A., Michéa, D., and Malet, J.-P.: Improved co-registration of Sentinel-2 and Landsat-8
958 imagery for earth surface motion measurements, *Remote Sensing*, 10(2), 160, doi:
959 10.3390/rs10020160, 2018.

960 Takaku, J., Tadono, T., and Tsutsui, K.: Generation of high resolution global DSM from ALOS
961 PRISM, *ISPRS International Archives of the Photogrammetry, Remote Sensing and Spatial In-*
962 *formation Sciences*, Vol. XL-4, 243-248, 2014.

963 Vaughan, D. G., Comiso, J. C., Allison, I., Carrasco, J., Kaser, G., Kwok, R., Mote, P., Murray, T.,
964 Paul, F., Ren, J., Rig- not, E., Solomina, O., Steffen, K., and Zhang, T.: Observations: Cry-
965 osphere, in: *Climate Change 2013: Physical Science Basis. Contribution of Working Group I*
966 *to the Fifth Assessment Report of the Intergovernmental Panel on Climate Change*, edited by:
967 Stocker, T. F., Qin, D., Plattner, G.-K., Tignor, M., Allen, S. K., Boschung, J., Nauels, A., Xia,
968 Y., Bex, V., and Midgley, P. M., Cambridge University Press, Cambridge, United Kingdom
969 and New York, NY, USA, 317-382, 2013.

970 Wouters, B., Gardner, A.S., and Moholdt, G.: Global glacier mass loss during the GRACE satellite
971 mission (2002-2016), *Frontiers in Earth Science*, 7 (96), doi: 10.3389/feart.2019.00096, 2019.

972 Zemp, M., [Hoelzle, M., and Haeberli, W.: Distributed modelling of the regional climatic equilibri-](#)
973 [um line altitude of glaciers in the European Alps, *Global and Planetary Change*, 56, 83–100,](#)
974 [2007.](#)

975 [Zemp, M.,](#) Paul, F., Hoelzle, M., and Haeberli, W.: Alpine glacier fluctuations 1850-2000: An
976 overview and spatio-temporal analysis of available data and its representativity. In: Orlove, B.,
977 Wiegandt, E. and Luckman, B. (eds.): *Darkening Peaks: Glacier Retreat, Science, and Society*,
978 University of California Press, Berkeley and Los Angeles, 152-167, 2008.

979 Zemp, M., Frey, H., Gärtner-Roer, I., Nussbaumer, S.U., Hoelzle, M., Paul, F., Haeberli, W., Den-

980 zinger, F., Ahlstrom, A.P., Anderson, B., Bajracharya, S., Baroni, C., Braun, L.N., Caceres,
981 B.E., Casassa, G., Cobos, G., Davila, L.R., Delgado Granados, H., Demuth, M.N., Espizua, L.,
982 Fischer, A., Fujita, K., Gadek, B., Ghazanfar, A., Hagen, J.O., Holmlund, P., Karimi, N., Li,
983 Z., Pelto, M., Pitte, P., Popovnin, V.V., Portocarrero, C.A., Prinz, R., Sangewar, C.V., Sev-
984 erskiy, I., Sigurdsson, O., Soruco, A., Usabaliev, R., and Vincent, C.: Historically unprece-
985 dented global glacier changes in the early 21st century, *Journal of Glaciology*, 61 (228),745-
986 762, 2015.

987 Zemp, M., Huss, M., Thibert, E., Eckert, N., McNabb, R., Huber, J., Barandun, M., Machguth, H.,
988 Nussbaumer, S.U., Gärtner-Roer, I., Thomson, L., Paul, F., Maussion, F., Kutuzov, S., and
989 Cogley, J.G.: Global glacier mass changes and their contributions to sea-level rise from 1961
990 to 2016, *Nature*, 568, 382-386, 2019.

991

GI-ID	P1	STD%	P2	STD%	P3	STD%	P4	STD%	P5	STD%	Mean	STD%
1	9.37	1.89	8.96	0.18	8.40	0.79	8.77	0.99	8.64	3.86	8.83	4.14
2	6.50	2.10	6.08	1.31	6.07	1.43	5.95	0.81	6.25	1.31	6.17	3.48
3	0.79	3.75	0.72	3.51	0.65	1.62	0.73	0.74	0.71	8.77	0.72	7.02
5	4.10	3.03	3.22	2.33	3.50	3.92	3.45	5.66	3.45	7.46	3.54	9.33
6	2.88	1.82	2.83	1.52	2.90	3.32	2.75	2.69	2.91	1.86	2.85	2.27
7	1.20	1.04	1.06	6.10	1.16	2.71	1.14	1.91	1.20	2.90	1.15	4.81
8	5.35	0.24	5.13	1.58	5.25	0.77	5.24	0.31	5.26	1.24	5.25	1.51
9	2.75	0.43	2.75	1.64	2.59	3.80	2.72	2.17	2.64	1.53	2.69	2.64
10	0.38	6.38	0.30	2.76	0.25	4.37	0.30	3.39	0.25	4.80	0.30	17.24
11	0.28	12.40	0.27	0.64	0.26	2.06	0.26	1.71	0.30	8.69	0.27	6.77
12	0.24	1.41	0.25	4.34	0.20	3.30	0.21	5.54	0.23	6.79	0.23	8.85
13	0.08	41.67	0.12	17.80	0.03	8.00	0.08	17.68	0.11	17.65	0.08	44.21
14	0.21	4.29	0.17	15.52	0.11	16.16	0.20	5.03	0.21	13.42	0.18	24.01
15	0.12	4.96	0.12	7.10	0.11	1.09	0.11	14.22	0.14	3.45	0.12	11.01
Sum	34.25	1.48	31.97	0.97	31.48	1.13	31.90	0.91	32.31	2.72	32.38	3.35

1115

1116

1117

1118

Figure captions

1119

Fig. 1: Overview of the study region with footprints (colour-coded for acquisition year) of the Sentinel-2 tiles used (see Table 1 for numbers).

1120

1121

1122

Fig. 2: Comparison of hillshade views from a) the AW3D30 DEM and b) the TanDEM-X DEM for a region around the Mt. Blanc/Monte Bianco. Glacier outlines are shown in red, data voids in the TanDEM-X DEM are depicted as constantly grey areas. The AW3D30 DEM has been obtained from <https://www.eorc.jaxa.jp/ALOS/en/aw3d30/index.htm> and is provided by JAXA. The TanDEM-X DEM has been acquired by the TerraSAR-X/TanDEM-X mission and is provided by DLR (DEM_GLAC1823).

1128

1129

Fig. 3: Results of the automated (clean ice) glacier mapping and threshold selection. a) band ratio MSI band 4 / MSI band 11 (red/SWIR). b) Glacier classification results using different thresholds. The lower values add some additional pixels, in particular in shadow regions where the threshold is most sensitive. c) Blue band threshold to remove wrongly classified rock in shadow. The highest value has been used resulting in a good performance in the left part of the image (white arrow) and a bad one to the right (green arrow), where correctly classified ice in shadow is removed. d) Final outlines (light blue) on top of the Sentinel-2 image in natural colours. All Sentinel-2 images shown in the background: © Copernicus data (2016).

1137

1138

Fig. 4: Examples of challenging classifications in different countries. a) Debris cover delineation (red) around Grossvenediger (Hohe Tauern) in Austria with raw extents (light grey) and outlines from the previous national inventory (yellow). b) Tré-La-Tête Glacier (Mont-Blanc) with automatically derived glacier extents (green), manually corrected outlines from 2015 (red) and outlines

1139

1140

1141

1142 derived from aerial photographs taken in 2008 (yellow). The S2 image from August 2015 is in the
1143 background. c) Subset of the Orobic Alps in Italy (S2 image from September 2016), with evidence
1144 of topographic shadow and debris covered glaciers. The inset shows an aerial photograph with bet-
1145 ter glacier visibility but seasonal snow. d) S2 image from 2015 showing differences in interpreta-
1146 tion of debris cover for Gavirolas glacier in Switzerland for the inventories from 2003 (yellow),
1147 2008 (green) and 2015 (red). The inset shows a close-up of its lowest debris-covered part obtained
1148 from aerial photography for comparison (this image is a screenshot from Google Earth). All Senti-
1149 nel-2 images shown in the background: © Copernicus data (2016).

1150

1151 Fig. 5: Relative frequency histograms for glacier count and area per a) size class and b) aspect sec-
1152 tor for all glaciers.

1153

1154 Fig. 6: Glacier area vs. a) minimum and maximum elevation and b) elevation range for all glaciers.

1155

1156 Fig. 7: Spatial distribution of median elevation (colour coded) for glaciers larger 0.5 km². The inset
1157 shows a scatterplot depicting glacier aspect (counted from North at 0/360°) vs. median elevation
1158 [and values averaged for each cardinal direction](#).

1159

1160 Fig. 8: Normalised glacier hypsometry per country as derived from the AW3D30 DEM.

1161

1162 Fig. 9: Visualisation of the strong glacier area shrinkage between 2003 (yellow) and 2015 (red) for
1163 a sub-region of the Zillertal Alps (Austria and Italy). Sentinel-2 image shown in the background: ©
1164 Copernicus data (2016).

1165

1166 Fig. 10: Overlay of glacier outlines from 2003 (black) and 2016 (yellow) showing the different
1167 interpretation of glacier extents for the region around Sonnblückkees (SBK) in Austria. Sentinel-2
1168 image shown in the background: © Copernicus data (2016).

1169

1170 Fig. 11: Overlay of glacier outlines from the multiple digitising experiment by all participants.
1171 Colours refer to the first (yellow), second (red), third (green) and fourth (white) round of digitisa-
1172 tion. Sentinel-2 image shown in the background: © Copernicus data (2016).

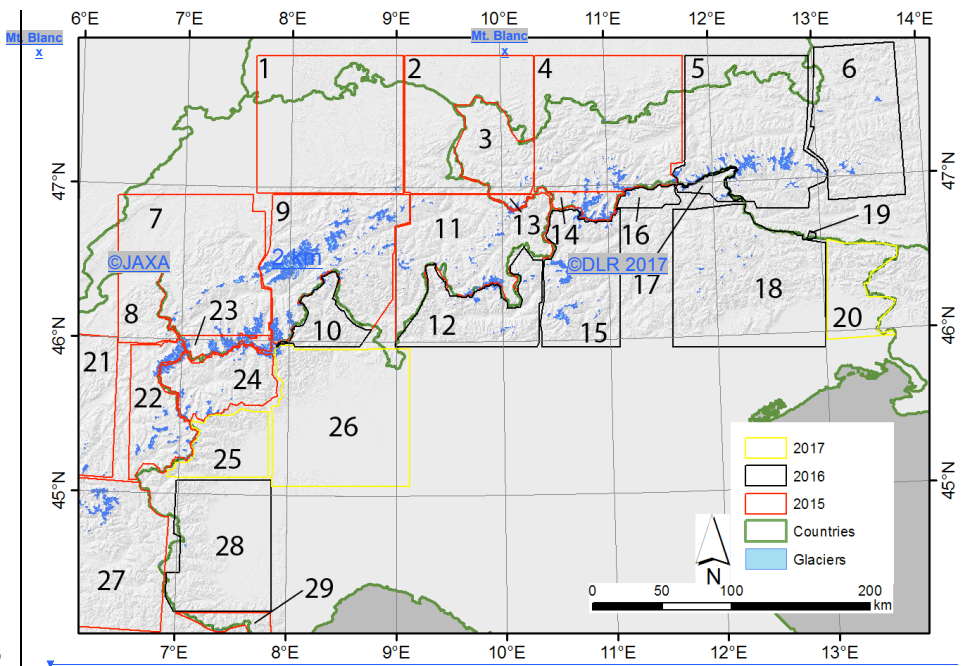
1173

b)

1174

Figures

1175



1176

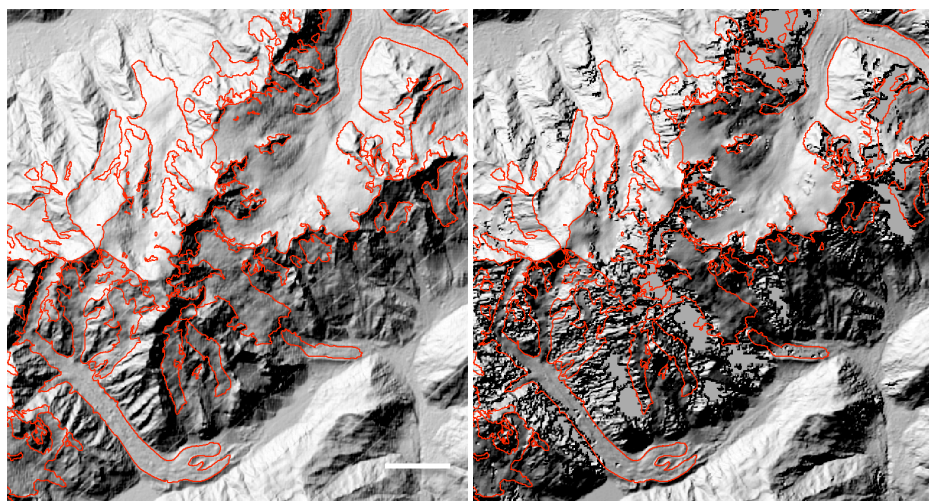
Figure 1

1177

1178

1179

fp 28 4 20 3:19 PM
Deleted: ... [8]



1180

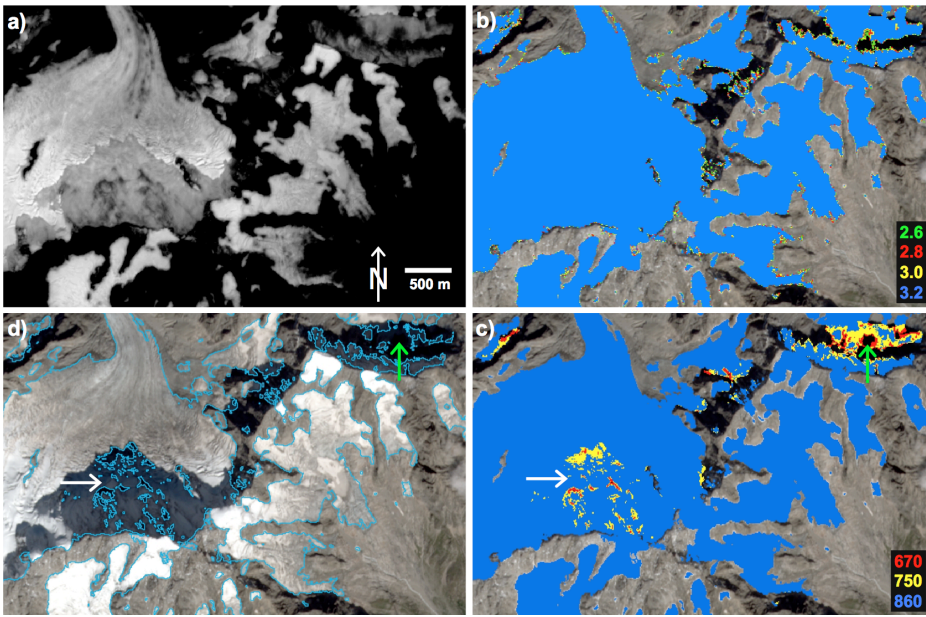
Figure 2

1182

1183

fp 28 4 20 3:19 PM
Deleted: <sp><sp> ... [9]

1188



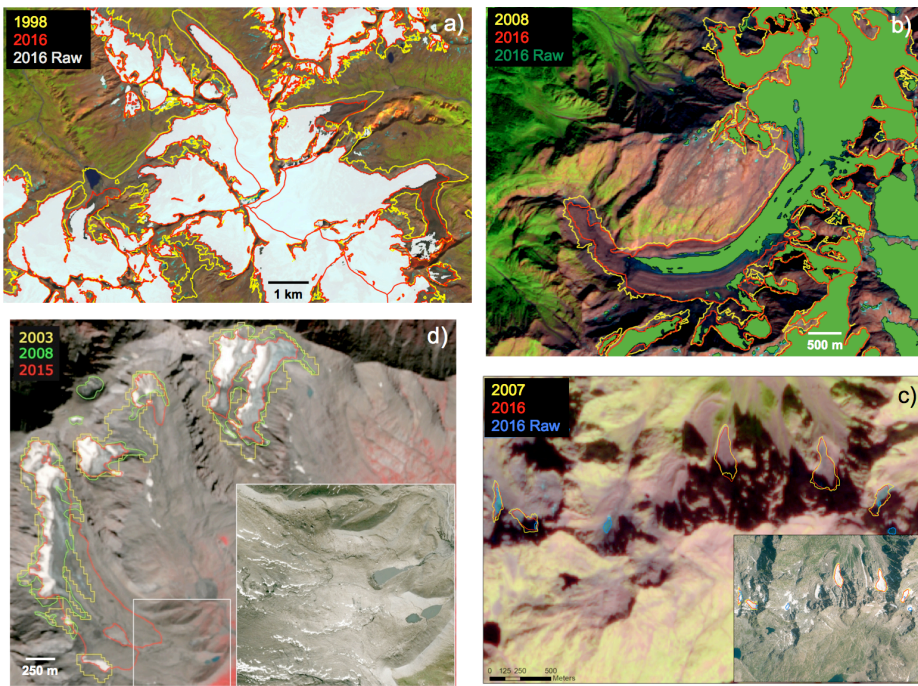
1189

1190

Figure 3

1191

1192



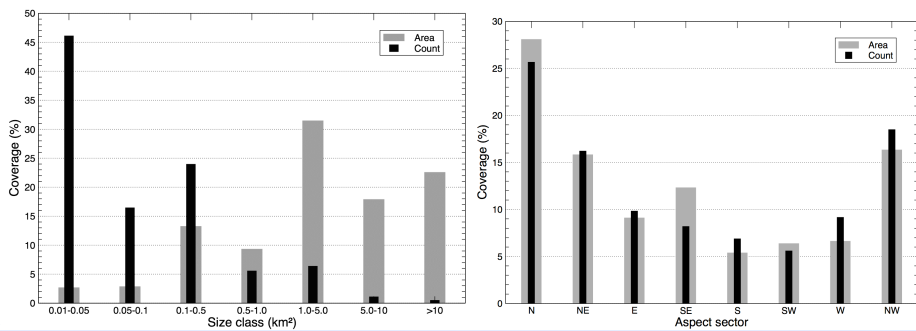
1193

1194

Figure 4

1195

1196



fp 28 4 20 3:19 PM
Deleted: <sp><sp>

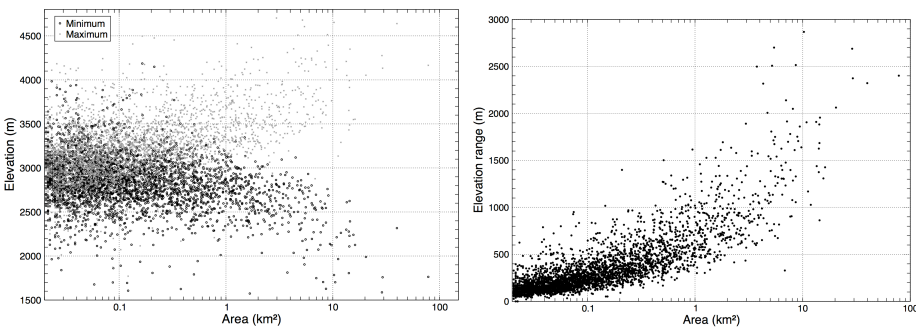
1197

1198

Figure 5

1199

1200



fp 28 4 20 3:19 PM
Deleted: <sp><sp>

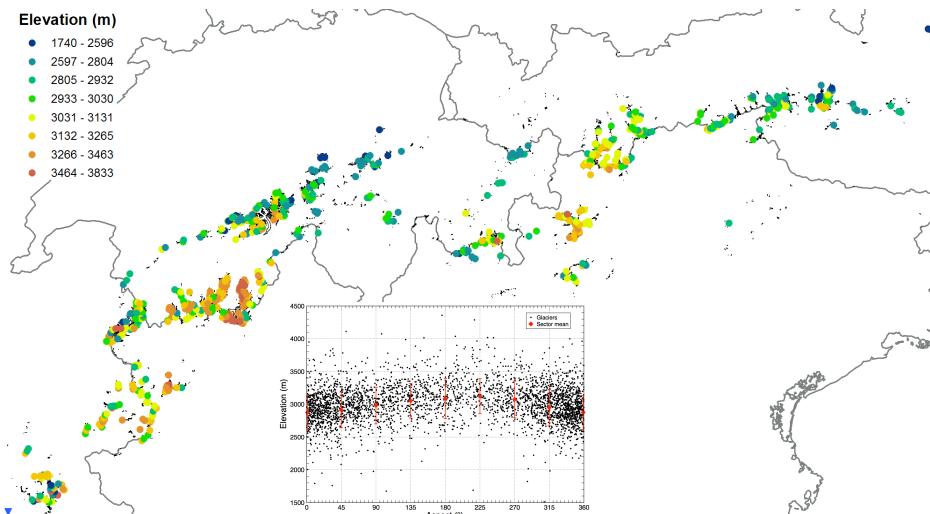
1201

1202

Figure 6:

1203

1204



fp 28 4 20 3:19 PM
Deleted: <sp>

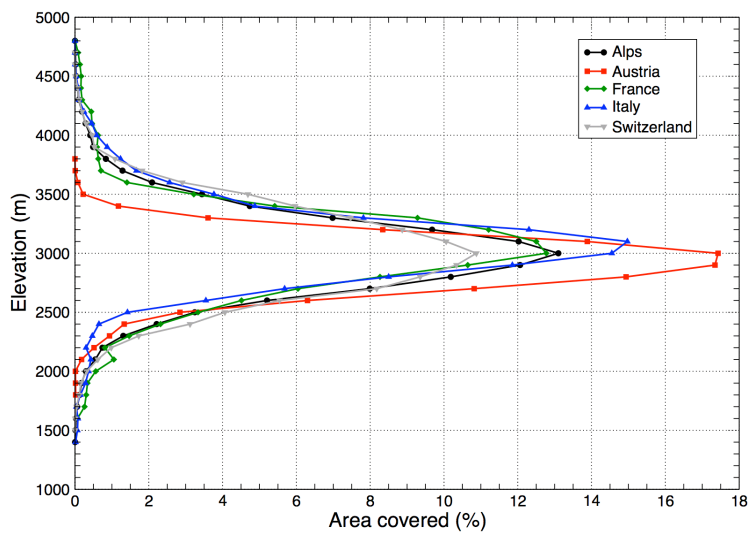
1205

1206

Figure 7

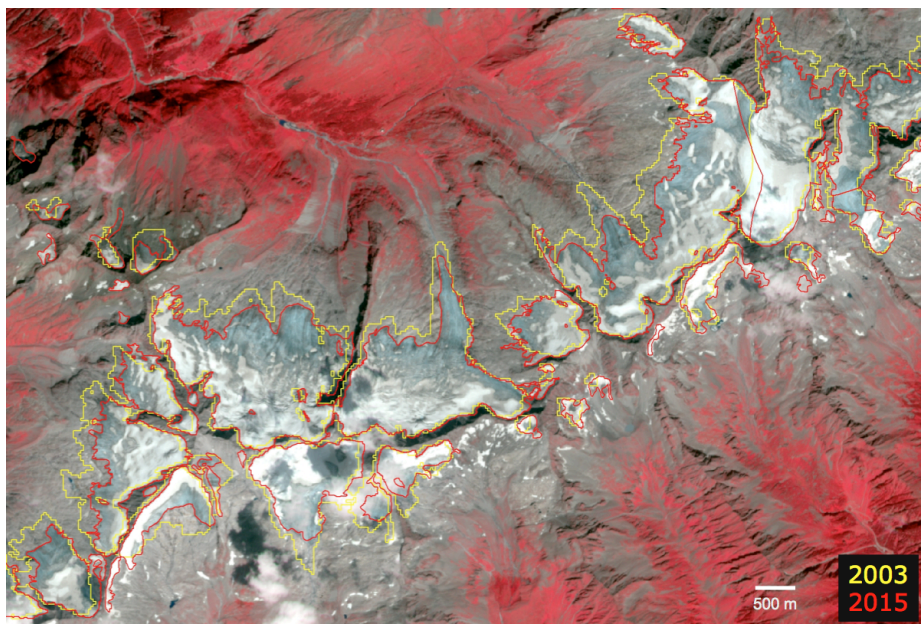
1207

1211
1212

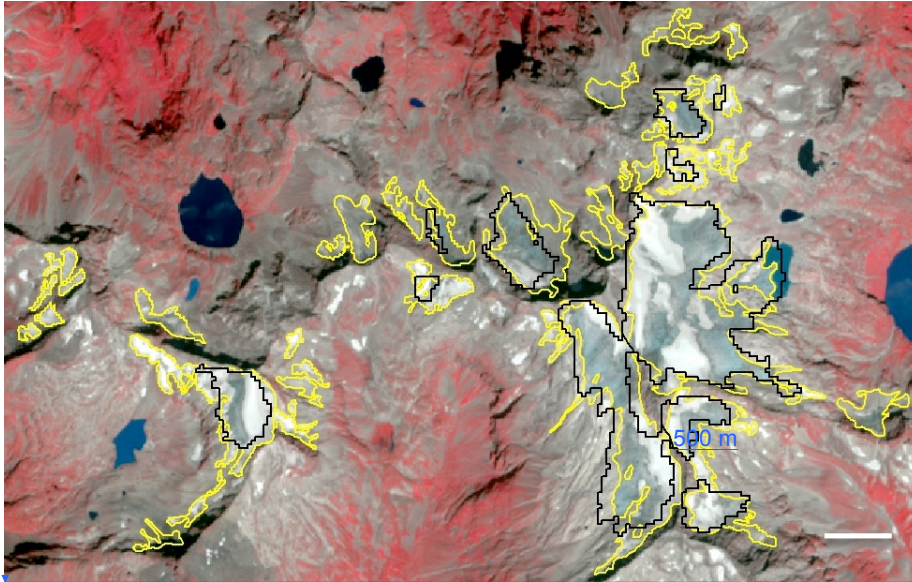


1213
1214 Figure 8

1215
1216
1217



1218
1219 Figure 9
1220

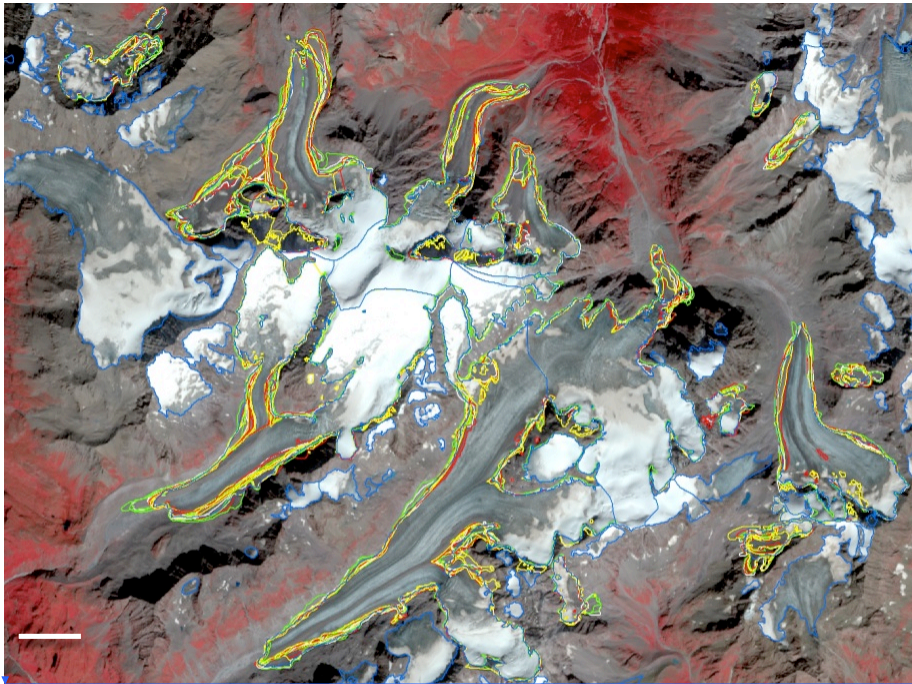


fp 28 4 20 3:19 PM
 Deleted: <sp><sp>

km

1221
 1222
 1223
 1224

Figure 10



fp 28 4 20 3:19 PM
 Deleted: <sp><sp>

1225
 1226
 1227

Figure 11